HHS Public Access

Author manuscript

ACS Nano. Author manuscript; available in PMC 2016 July 05.

Published in final edited form as:

ACS Nano. 2016 January 26; 10(1): 930–937. doi:10.1021/acsnano.5b06066.

Mussel-Inspired Anchoring of Polymer Loops That Provide Superior Surface Lubrication and Antifouling Properties

Taegon Kang[†,‡,∥,▲], **Xavier Banquy**[†,§,⬡], **Jinhwa Heo**[†,‡], **Chanoong Lim**[⊥], **Nathaniel A. Lynd**[†], **Pontus Lundberg**[†], **Dongyeop X. Oh**[#], **Han-Koo Lee**[¶], **Yong-Ki Hong**[△], **Dong Soo Hwang**[*,⊥,#,▼], **John Herbert Waite**[*,†,‡], **Jacob N. Israelachvili**[*,†,§], and **Craig J. Hawker**[*,†,‡]

[†]Materials Research Laboratory, University of California, Santa Barbara, California 93106, United States

[‡]Materials Department, University of California, Santa Barbara, California 93106, United States

[§]Department of Chemical Engineering, University of California, Santa Barbara, California 93106, United States

[∥]Chemical Research Institute, Samsung SDI Inc., Gocheon-Dong, Uiwang-Si, Gyeonggi-Do 437-711, Republic of Korea

[⊥]School of Interdisciplinary Bioscience and Bioengineering, Pohang University of Science and Technology, Pohang 790-784, Republic of Korea

[#]Ocean Science and Technology Institute, Pohang University of Science and Technology, Pohang 790-784, Republic of Korea

[¶]Pohang Accelerator Laboratory, Pohang University of Science and Technology, Pohang 790-784, Republic of Korea

[▼]Division of Integrative Biosciences and Biotechnology, School of Environmental Science and Engineering, Pohang University of Science and Technology, Pohang 790-784, Republic of Korea

[△]Department of Biotechnology, Pukyong National University, Busan 608-737, Republic of Korea

Abstract

We describe robustly anchored triblock copolymers that adopt loop conformations on surfaces and endow them with unprecedented lubricating and antifouling properties. The triblocks have two end blocks with catechol-anchoring groups and a looping poly(ethylene oxide) (PEO) midblock. The loops mediate strong steric repulsion between two mica surfaces. When sheared at constant speeds of ~2.5 μm/s, the surfaces exhibit an extremely low friction coefficient of ~0.002–0.004 without

[*]Corresponding Authors: dshwang@postech.ac.kr. waite@lifesci.ucsb.edu. jacob@engr.ucsb.edu. hawker@mrl.ucsb.edu.

[▲]Author Contributions

T.K. and X.B. contributed equally.

[⬡]Present address

Faculty of Pharmacy, Université de Montréal, C.P. 6128, Succursale Centre Ville, Montréal, Quebec H3C 3J7, Canada.

Notes

The authors declare no competing financial interest.

Supporting Information

The Supporting Information is available free of charge on the ACS Publications website at DOI: 10.1021/acsnano.5b06066.
Materials and general procedures, instrumentation, abbreviations, synthesis, friction test, NEXAFS test, and antifouling test (PDF)

any signs of damage up to pressures of ~2–3 MPa that are close to most biological bearing systems. Moreover, the polymer loops enhance inhibition of cell adhesion and proliferation compared to polymers in the random coil or brush conformations. These results demonstrate that strongly anchored polymer loops are effective for high lubrication and low cell adhesion and represent a promising candidate for the development of specialized high-performance biomedical coatings.

Graphical Abstract

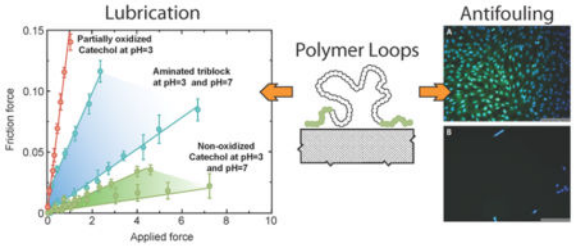

Keywords

polymer loops; lubrication; antifouling; catechol; surface forces apparatus

Advanced biomedical devices such as implants or sensors often require complex chemical modifications of their surfaces for proper performance.[1–3] A representative example of such modification consists of grafting polymer brushes to provide surfaces with good lubrication or antifouling properties.[4–7] Ocular lenses and articular implants represent two of the numerous applications requiring both good lubrication and antifouling properties to the material surfaces but continue to pose significant engineering challenges to fabrication.

Development of polymer coatings for functional surfaces, such as articular implants, requires strong anchoring of the polymer to the surface in order to withstand high loads and shear stresses under physiological conditions. Today, chemically grafted polyelectrolyte brushes are the only known synthetic system able to impart good lubrication under physiological conditions;[4,8] however, the costly and complicated processing involved in this approach—as well as the sensitivity of polyelectrolytes or even zwitterionic polymers to the ionic strength of the medium—is a severe drawback for their future use in biomedical applications.[4]

On the other hand, the antifouling properties of polar neutral polymer brushes have been shown to be superior to that of polyelectrolyte brushes due to their insensitivity to the ionic strength of the medium, but these brushes typically perform poorly as lubricants under physiological conditions.[8,9]

Combining good lubrication/wear resistance and antifouling properties requires the use of innovative polymers that can be tethered to surfaces to withstand removal during shear and also maintain low interpenetration of polymers or proteins in order to efficiently lubricate the surfaces and prevent adhesion of proteins and fouling precursors.

Polymer loops have been suggested as a good alternative to polymer brushes for their ability to maintain lower interpenetration of polymer chains under normal load compared to their equivalent in the brush conformation.[10] Lubricating protein Lubricin, found in mamalian's articular joints, is known to adopt the loop conformation and has also demonstrated excellent antifouling properties.[11–13] Previous studies using triblock copolymers with two flanking adhesive blocks and a nonadhesive middle block have been shown to adopt the loop conformation when adsorbed to a surface.[14,15] However, due to their weak adhesion to target surfaces, the systems investigated to date lack the performance levels to justify their translation to medical devices.[15]

In order to further investigate these issues, we have prepared bioinspired triblock copolymers *via* a simple preparation route that adsorb to model surfaces in the loop conformation. The triblock copolymers have a neutral poly(ethylene oxide) (PEO) middle block which provides good lubrication and antifouling properties for the surfaces[6,7,16–18] and two catechol-functionalized end blocks, adopted from mussel adhesive proteins, which strongly anchor the polymer to most mineral, metallic, and polymeric (hydrophilic and hydrophobic) surfaces.[17,19] A mussel adhesive protein, known as mfp-2, has a similar triblock structure with a middle block consisting of 11 repeats of an epidermal growth factor motif and two catechol (DOPA)-rich end blocks.[20]

RESULTS AND DISCUSSION

Figure 1 depicts the synthetic strategy of the triblock polymer starting with the catechol-functionalized poly(ethylene oxide)-based triblock copolymer. Eugenol (**1**) was selected as the precursor of the catechol due to its commercial availability and because it can be protected quantitatively under ambient conditions using tris(pentafluorophenyl)borane (TPFPB)-catalyzed silylation with triethylsilane (**2**). As previously reported,[20] TPFPB-catalyzed silylation, reaction between **1** and **2**, was carried out to completion at room temperature under ambient conditions. **3** was converted to a thiol (**5**) *via* a thiol–ene coupling reaction with ethanedithiol (**4**). The PEO-based triblock copolymer, P(EO-*co*-AGE)-*b*-PEO-*b*-P(EO-*co*-AGE), was synthesized by the anionic ring-opening copolymerization of ethylene oxide (EO) and allyl glycidyl ether (AGE) from a PEO macroinitiator in THF at 45 °C. The prepared silyl-protected catecholic monomer (**5**) was then used to functionalize the P(EO-*co*-AGE)-*b*-PEO-*b*-P(EO-*co*-AGE) triblock copolymers (**9**) through a simple thiol–ene reaction by exposure to 365 nm light for 30 min in the presence of 2,2-dimethoxy-2-phenylacetophenone as a photochemical initiator.[21] The silyl-protected catechol-functionalized triblock copolymer (**8**) was obtained in quantitative yield without any observable silyl deprotection or allyl groups remaining.

In order to characterize the conformation of the catechol-functionalized triblock copolymers on silicon-oxide-based surfaces, we measured the interaction forces between two mica surfaces bearing adsorbed catechol-functionalized triblock copolymer chains using the surface forces apparatus (SFA). The copolymer was adsorbed on atomically flat mica surfaces from a concentrated solution (100 mg/mL) in 0.2 M sodium acetate buffer at pH 3. After the surfaces were rinsed with the same buffer to remove any nonadsorbed material, the normal interaction forces, F, between the surfaces were measured as a function of the

separation distance, D, in polymer-free acetate buffer (0.2 M, pH 3). As shown in Figure 2, when the triblock copolymer is adsorbed at pH 3—the condition under which the catechol moieties are activated by deprotection of the silyl — groups without any further oxidation of the catechols the interaction force profiles present the sigmoid S-shaped characteristic of surface-anchored polymers in the brush/loop conformation.[22,23] The onset of the interaction starts at 110–120 nm (see Figure 2B), which corresponds approximately to a polymer layer of 55–60 nm thickness on each surface. Since the R_h of the polymer, as measured by dynamic light scattering, is approximately 20 nm, and the fully extended length of the polymer is 236 nm (166 nm for the middle block and 35 nm for the lateral blocks), it is likely that the polymer adopts a loop conformation on the surfaces similar to the one depicted in Figure 2A.

The interaction forces between polymer loops adsorbed on a surface are similar to the interaction forces between two surfaces bearing polymer brushes. We used the Alexander–de Gennes[24] (AdG) equation to fit the experimental data.

$$F/R=\frac{16kTL}{35s^3}\left[7\left(\frac{2L}{D}\right)^{5/4}+5\left(\frac{D}{2L}\right)^{7/4}-12\right] \quad (1)$$

We obtain a grafting distance of s = 5–10 nm and a brush height of L = 68 nm, which corresponds to 80% of the fully extended length of half of the middle block.

The choice of the AdG model was guided by recent experimental studies that have shown that the segment volume fraction density of loops can be accurately described using the pseudo brush model,[25] and interaction force measurements between plates bearing loops showing than the loop height and the interaction forces can be described (to some extent) using the AdG model of a pseudo brush.[11,14,26] We are aware that such an approach still neglects some intrisic properties of the polymer loops, such as their curvature and overlap with neighbors. To our knowledge, these effects have not yet been considered in theoretical studies.

These results confirm that the strong affinity of the catechol moieties to the mica stabilizes the polymer in the loop conformation even at this relatively high grafting density. Confirmation of the loop conformation was obtained by NEXAFS analysis (see Supporting Information Figure S2). Two conclusions may be drawn from this analysis. First, the catechol groups are not present in the distal part of the polymer layer, and therefore, free lateral blocks are absent; second, the catechol group adopts a vertical upright orientation on the substrate, suggesting coordinative interactions between the catechol and the substrate (see Supporting Information Figure S2).

To separate the surfaces, the forces remain purely repulsive, independent of the contact time (up to 1 h), confirming that no interpenetration or bridging of the surfaces by free dangling polymer chains (tails) occurred. The slight hysteresis observed in Figure 2 could originate from a dynamic effect due to a high separation speed of the surfaces. The additional force

profiles provided in the Supporting Information show that this hysteresis is, in fact, quite small and occurs in the low-force/ long-range portion of the force profiles, only suggesting that it appears by the slow flow of the liquid back between the surfaces.

As a control experiment, the polymer was adsorbed from an acetate buffer solution at pH 5, which is known to favor the oxidation of the catechol functional group to *o*-quinone.[27] The polymers, which now have *o*-quinone moieties at the end blocks, were expected to have much less affinity to the mica surface and to adopt a random coil conformation on the surface. The interaction force profiles measured under these conditions indeed showed that the conformation of the polymer on the mica surface had changed, as seen from the purely exponential shape of the interaction curve. The onset of the interaction forces was now found to be 40 nm (Figure 2B), which corresponds to the thickness of two polymer layers in a random coil conformation on the surface. On separation, the interaction forces now showed an adhesive minimum, suggesting that the polymer surface coverage is now low enough to allow the formation of weakly adhesive polymer chain bridges between the surfaces.

The extreme sensitivity of the polymer conformation to the pH of the solution on adsorption also affects the lubricating properties of the surfaces. When adsorbed at pH 3, the polymer layer presents excellent lubricating properties independently of the pH of the medium, as shown in Figure 3. The measured friction coefficient, $\mu = F/L$, was found to vary between 0.002 ± 0.001 and 0.004 ± 0.001 in the pH range from 3 to 7. These values are much lower than what has been reported so far for PEO brushes[28,29] or neutral polymer loops weakly anchored on mica[15] and are comparable to strongly adsorbed polyelectrolyte and zwitterionic brushes under similar ionic strengths and normal pressures.[4] Interestingly, once the polymer is strongly adsorbed on the surface, its lubricating proper properties are independent of the medium pH, in contrast to polyelectrolyte and zwitterionic polymers. This is expected since the polymer is electrostatically neutral and the bidentate mode of adsorption by the catechol is known to have a very stable surface-binding lifetime.[19]

When the anchoring groups of the polymer end blocks are not strong enough to attach to mica, as occurs after catechol oxidation at pH 5, the measured friction coefficient is found to be more than an order of magnitude higher ($\mu = 0.074 \pm 0.002$ when adsorbed at pH 5 and measured at pH 3, same as in Figure 2B). Similar results were obtained when the catechol side chains were replaced by amine groups. Amine groups are known to adsorb strongly on negatively charged mica surfaces at pH 3 *via* electrostatic interactions (“ionic bonds”). This strong interaction is able to stabilize the polymer in a loop conformation, and good lubrication was indeed measured under such conditions (Figure 3B), even though it seems to be much less efficient than the catechol-functionalized polymer. When the pH was increased from 3 to 7, the measured friction coefficient increased, as well, from 0.008 to 0.027, which is more than a 3-fold increase. This marked sensitivity to pH changes recapitulates the weakness of the electrostatic interaction between amine anchoring compared to catechol functionality.

We finally compared the performance of the catechol-functionalized triblock polymers with equivalent diblock polymers having the same anchoring block as the previous triblocks and a

pure PEO block with half the length of the triblock middle block. The surfaces were treated with a diblock solution as described earlier (for adsorption at pH 3). The surfaces showed very good lubrication up to a normal applied force of 0.1 mN at pH 3 ($\mu = 0.007 \pm 0.006$) and 0.75 mN at pH 7 ($\mu = 0.007 \pm 0.006$; see Figure 3C) and then exhibited a 100-fold increase in the friction coefficient at higher normal forces due mostly to the development of damage in the polymer layers.

These results clearly show that polymer loops substantially reduce frictional forces between the surfaces compared with polymer brushes, mainly by reducing interpenetration.

Antifouling properties of the catechol-functionalized triblock copolymer against mammalian cells (MC-3T3) and marine red alga (*Porphyra suborbiculata*) were also tested. For the mammalian cell experiment, MC-3T3 cells (preosteoblast) were chosen since they can induce calcium-phosphate-based biomineralization during settlement and proliferation on a biomedical surface,[30] thereby increasing the surface roughness and altering lubricating properties. As a control, MC-3T3 cells on uncoated glass surfaces showed normal adhesion and proliferation (Figure 4A). In stark contrast to the control, most cells deposited on a catechol-functionalized triblock copolymer-coated surface were found to be small and round-shaped and could be easily washed away when the surfaces were transferred to another medium, which indicates that MC-3T3 cells do not adhere, spread, and proliferate on the triblock copolymer-coated surfaces. Only a few adherent cells were observed by fluorescence microscopy on the entire coated surface (Figure 4B). To quantitatively measure MC-3T3 cell viability and proliferation, WST-8 (2-(2-methoxy-4-nitrophenyl)-3-(4-nitrophenyl)-5-(2,4-disulfophenyl)-2*H*-tetrazolium, monosodium salt)-based cell counting assay was performed. WST-8 produced yellow-colored product (formazan) when reduced by dehydrogenases in living cells.[31] As expected, the levels of cell viability and proliferation on catechol-functionalized triblock copolymer-coated surfaces were much less than those on bare glass surfaces or on surfaces coated with homopolymers of PEO, demonstrating that the catechol-functionalized triblock copolymer effectively blocked cell adhesion on the surface (Figure 4C). Importantly, cell viability on the triblock copolymer-coated surface monotonically decreased with the incubation time, whereas tests with control surfaces showed a constant increase of cell viability. Moreover, the antifouling properties of the polymer-coated surfaces were not reduced by submitting the surfaces to intense sonication, indicating that catechol-mediated anchoring withstands significant and longstanding mechanical stresses (Figure 4C).

Catechol moieties are prone to oxidation at physiological pH conditions and react readily with various amines or thiols functional groups present on the extracellular side of cells membrane proteins.[18,32] Therefore, the minimal adhesion exhibited by cells on the catechol-functionalized polymer substrate reveals that most of the catechol moieties of the end blocks are anchored to the surface. Dangling nonadsorbed catechol moieties oxidized to *o*-quinones should not therefore be available for attachment to the cells.

Control homopolymers of PEOs (8 and 900 kDa) did not show any antifouling properties based on the cell viability tests (Figure 4C), reinforcing the fact that anchoring moieties are essential for good antifouling properties.

The antifouling ability of the catechol-functionalized triblock copolymer in marine environment was briefly tested against the marine red alga *Porphyra suborbiculata* spores. Catechol-functionalized triblock copolymer-coated glass surfaces blocked the attachment of algal spores as well as cells with rhizoids (Figure S3). In contrast to poly-L-lysine-mediated anchoring,[7,28] catechol-mediated immobilization can be applied to a variety of surfaces, including metals, plastics, and ceramics, thanks to the versatile wet adhesion ability of catechol.

CONCLUSIONS

Our results demonstrate that the synthesized triblock copolymer combines excellent lubricating and antifouling properties under a wide range of experimental conditions. The simple adsorption step necessary to coat the surfaces makes it very attractive for the future development of functional biomaterials for applications in prosthetic devices and bioMEMs.

METHODS

Materials

Unless otherwise stated, ACS reagent grade chemicals and solvents were purchased from Sigma-Aldrich and used without further purification. Tetrahydrofuran was collected from a dry solvent system and used immediately thereafter. Allyl glycidyl ether was purchased from TCI-America, Inc., degassed by freeze–pump–thaw, and distilled onto butylmagnesium chloride (Sigma-Aldrich), where it was stirred for 10 min at 0 °C and distilled to a buret for use. Potassium naphthalenide was prepared from potassium metal and recrystallized naphthalene in dry THF and allowed to stir with a glass-coated stir bar for 24 h at room temperature before use. Triethylsilane and tris(pentafluorophenyl)borane were purchased from Gelest. 2,2-Dimethoxy-2-phenylacetophenone (99%), eugenol, ethane dithiol, ethylene oxide (99.5%+), and poly(ethylene oxide) were purchased from Sigma-Aldrich. Deuterated solvents for NMR were purchased from Cambridge Isotope Laboratories, Inc.

Instrumentation

^{1}H and ^{13}C NMR spectra were recorded on Varian 600 or Bruker AC 500 spectrometers as indicated. Chemical shifts are reported in parts per million (ppm) and referenced to the solvent. The lamp used for irradiation of samples was a UVP Black Ray UV Bench Lamp XX-15L, which emits 365 nm light at 15 W. Mass spectral data were collected on a Micromass QTOF2 quadrupole/ time-of-flight tandem mass spectrometer. Size-exclusion chromatography was performed on a Waters chromatograph with four Viscotek colums (two IMBHMW-3078, I-series mixed-bed high molecular weight columns and two I-MBLMW-3078, I-series mixed-bed low molecular weight columns) for fractionation, a Waters 2414 differential refractometer and a 2996 photodiode array detector for detection of eluent, and chloroform with 0.1% tetraethylamine at room temperature was used as the mobile phase. Gas chromatography was carried out on a Shimadzu GC-2014 using a flame ionization detector and a Restek column (SHRXI-5MS) for separation.

Friction Test

Substrate Preparation—Atomically smooth mica surfaces were freshly cleaved under a laminar flow hood and immediately deposited on another large freshly cleaved mica backing sheet for storage. In this way, the mica interface in adhesive contact with the backing sheet is kept free from dust contamination while the other interface can be coated with silver. The thickness of the mica sheets was 2.5–3.5 μm. The thickness of the silver coating was kept constant (55 nm) and deposited by Joule effect vapor deposition. Silvered mica sheets were glued, silvered side down, on silica cylindrical disks (2 cm curvature) using a hard epoxy glue (EPON 1004F from Exxon Chemicals).

Adsorption of Triblock Polymers on Mica Surfaces—After the surface in the SFA was mounted, the apparatus was purged with dry nitrogen for 1 h in order to eliminate adsorbed water on the mica and to decrease the humidity of the surrounding atmosphere. After the thickness of the mica surfaces was measured by bringing them into adhesive contact, the surfaces were separated and a droplet of polymer solution of 100 μg/mL (pH 3) was introduced between them. The bottom part of the apparatus was then filled with the same buffer solution as the polymer solution in order to maintain saturated conditions and avoid evaporation of the polymer droplet solution during the adsorption process. After 1 h of adsorption, the polymer solution was removed and surfaces were abundantly rinsed with buffer solution at pH 3.

Measuring Interaction Forces Using the Surface Forces Apparatus—The SFA model 2000[33] was used in this study for accurate force–distance measurements. The top surface was installed on a recently developed 3D sensor actuator device that allows for displacement in the normal and lateral direction to be controlled with nanometer resolution as well as to simultaneously measure dynamic interaction forces in three dimensions (normal and lateral forces).

During a typical experiment, the separation distance between the two surfaces is measured using optical interferometry:[34] a white light beam is shined through the surfaces, and the interference fringes generated from the reflections of the light beam between the two silvered mica sheets are analyzed in a spectrometer equipped with a digital camera (Hamamatsu Orca 03G, USA). The separation distance D between the surfaces is calculated (to ±1 Å) from the wavelength of the interference fringes (also called fringes of equal chromatic order, FECO)[34]

The normal interaction force function $F(D)$ between the polymer-coated surfaces as a function of the separation distance D was obtained by measuring the deflection of the double cantilever spring supporting the lower surface.[35–37] The real contact area—with a resolution of 1 μm—can be extracted from the analysis of the FECO fringes.[38]

Any localized defects, such as an initial sign of wear during shearing, can be precisely visualized, quantitatively measured, and monitored using the FECO technique as a function of time and normal force (or pressure).

NEXAFS Test

Iron oxide (Fe_2O_3) and titanium oxide (TiO_2) were used as the substrates as alternatives for mica, a kind of Si/Fe/Ti/O composite. The substrates were coated as follows. The triblock copolymer was dissolved as 1 mg/mL in 0.1 M acetic acid (aqueous). The solution was stirred for 1 h to deprotect silyl groups and filtered with a 0.2 μm syringe filter. Both substrates were immersed in the solution for 48 h, then vigorously washed with distilled water, and dried in vacuum oven overnight. The NEXAFS experiments were performed at the 2A undulator beamline at the Pohang Accelerator Laboratory in Korea. The total energy resolution was about 100 meV with a beam size of 0.5 mm × 0.2 mm. A linearly polarized X-ray beam was irradiated on the sample at 30 and 90° of the two different incidence angles (θ) between surface normal and light polarization (E-vector). All data were simultaneously collected in the total electron yield (TEY) and the partial electron yield (PEY) modes by recording the current to ground. Then the data were normalized to the beam current using a grid located upstream of the beamline. The experimental environment was maintained at room temperature and a base pressure of ~10^{-10} Torr. Both TEY and PEY mode NEXAFS techniques have been known as surface-sensitive tools. It is worth noting that PEY mode acquires more surface-sensitive electron signal (~1 nm of electron escape depth) than TEY mode (more than 10 nm of electron escape depth).[39,40]

Antifouling Test

Glass disks (R = 12 mm, thickness = 1 mm) were placed in glass dishes and incubated with 1 mg/mL of PEO, catechol-functionalized triblock copolymer (**10**) without iron, and **10** with $FeCl_3$ in TFA for 24 h. Unbound polymers and solvents were washed away by two incubations with the sample-coated surfaces in PBS (Hyclone) for 2 h and sonication for 30 s. The polymer coating on glass disks were confirmed by SEM images after polymer deposition. Uncoated glass disks were used as controls. Antifouling properties of the catechol-functionalized triblock copolymer against mammalian cells (MC-3T3) and marine red alga (*Porphyra suborbiculata*) were tested. The mouse preosteoblast cell line, MC3T3-E1 (Riken, Japan), was maintained in minimal essential medium-alpha (MEM-α; Hyclone) with 10% (v/v) fetal bovine serum (FBS; Hyclone) and 1% penicillin/streptomycin (Hyclone) at 37 °C in a humidified atmosphere of 5% CO_2 and 95% air. The subconfluent cells were detached by 0.25% trypsin-EDTA (Hyclone), and the viable cells were counted by trypan blue assay with hemocytometer. Cells (5×10^4, >95% viable) in MEM-α with 10% FBS were placed on each sample-coated glass disks, which were placed in a 24-well plate to test antifouling activity. For a quantitative measurement of cell number, cell counting kit-8 (CCK-8; Dojindo Laboratories, Japan) solution, which contains 2-(2-methoxy-4-nitrophenyl)-3-(4-nitrophenyl)-5-(2,4-disulfophenyl)-2*H*-tetrazolium (WST-8), produced a highly water-soluble formazan dye (yellow) upon reduction in the presence of an electron carrier from the viable cells. One to three days after cell seeding, 250 μL of CCK-8 was added to the wells to allow the formation of formazan crystals for 3 h at 37 °C. Finally, absorbance was measured at 450 nm using a microplate reader (Bio-Rad). For fluorescence microscopy, the cells were fixed with 4% (v/v) paraformaldehyde and permeabilized with 0.1% (v/v) Triton X-100. For nucleus staining, fixed cells were washed with PBS and immersed in 0.001% (w/v) 4′,6-diamidino-2-phenylindole. The fixed cells were washed

again with PBS and incubated 0.001% (w/v) with fluorescein isothiocyanate conjugated phalloidin containing PBS for 20 min to stain actin filaments of the cells. Finally, cells were fixed with Lisbeth's embedding medium (30 mM Tris-Cl, pH 9.5, 70% glycerol, 50 mg/ mL *N*-propyl gallate) and examined by fluorescence microscopy. Monospores of *Porphyra suborbiculata* Kjellman were collected from the intertidal zone of the rocky shore at Cheongsapo, Busan, S. Korea. Axenic isolation and culturing of the monospores were performed by following previous studies. Approximately, 200 spores in Provasoli's enriched seawater medium were placed on each sample-coated glass disk, which placed in a 24-well plate to test antifouling activity at 20 °C. One to seven days after spore seeding, attached spores or attached alive cells hatching from the spore attached on the surfaces were scraped, and the number of spores were counted under a microscope.

Supplementary Material

Refer to Web version on PubMed Central for supplementary material.

Acknowledgments

D.S.H. and X.B. thank the Santa Barbara Foundations through the Otis Williams Fellowship for financial support. X.B. thanks the Canadian Research Chair program and NSERC for financial support. D.S.H., C.L., and D.X.O. thank the National Research Foundation of Korea Grant (NRF-C1ABA001-2011-0029960). All the NEXAFS measurements were performed at room temperature at the 4D beamline of the Pohang Light Source II (PLSII). J.N.I. also thanks the Institute for Collaborative Biotechnologies through the U.S. Army Research Ofice (Contract W911NF-09-D-0001) for financial support, and J.N.I., J.H.W., and C.J.H. thank the MRSEC program of the National Science Foundation (DMR 1121053) for access to shared experimental facilities. This work was partially supported by the U.S. National Institutes of Health Award No. R01 DE018468.

References

1. Benz M, Chen NH, Israelachvili J. Lubrication and Wear Properties of Grafted Polyelectrolytes, Hyaluronan and Hylan, Measured in the Surface Forces Apparatus. J Biomed Mater Res. 2004; 71A:6–15.
2. Greene GW, Banquy X, Lee DW, Lowrey DD, Yu J, Israelachvili JN. Adaptive Mechanically Controlled Lubrication Mechanism Found in Articular Joints. Proc Natl Acad Sci U S A. 2011; 108:5255–5259. [PubMed: 21383143]
3. Stuart MAC, Huck WTS, Genzer J, Muller M, Ober C, Stamm M, Sukhorukov GB, Szleifer I, Tsukruk VV, Urban M, Winnik F, Zauscher S, Luzinov I, Minko S. Emerging Applications of Stimuli-Responsive Polymer Materials. Nat Mater. 2010; 9:101–113. [PubMed: 20094081]
4. Chen M, Briscoe WH, Armes SP, Klein J. Lubrication at Physiological Pressures by Polyzwitterionic Brushes. Science. 2009; 323:1698–1701. [PubMed: 19325108]
5. Xu FJ, Neoh KG, Kang ET. Bioactive Surfaces and Biomaterials *Via* Atom Transfer Radical Polymerization. Prog Polym Sci. 2009; 34:719–761.
6. Perrino C, Lee S, Spencer ND. End-Grafted Sugar Chains as Aqueous Lubricant Additives: Synthesis and Macrotribological Tests of Poly(L-Lysine)-Graft-Dextran (Pll-G-Dex) Copolymers. Tribol Lett. 2009; 33:83–96.
7. Perrino C, Lee S, Choi SW, Maruyama A, Spencer ND. A Biomimetic Alternative to Poly(Ethylene Glycol) as an Antifouling Coating: Resistance to Nonspecific Protein Adsorption of Poly(L-Lysine)-Graft-Dextran. Langmuir. 2008; 24:8850–8856. [PubMed: 18616303]
8. Raviv U, Giasson S, Kampf N, Gohy JF, Jerome R, Klein J. Lubrication by Charged Polymers. Nature. 2003; 425:163–165. [PubMed: 12968175]
9. Leckband D, Sheth S, Halperin A. Grafted Poly(Ethylene Oxide) Brushes as Nonfouling Surface Coatings. J Biomater Sci, Polym Ed. 1999; 10:1125–1147. [PubMed: 10591136]

10. Klein J. Entropic Interactions: Neutral and End-Functionalized Chains in Confined Geometries. J Phys : Condens Matter. 2000; 12:A19–A27.
11. Zappone B, Ruths M, Greene GW, Jay GD, Israelachvili JN. Adsorption, Lubrication, and Wear of Lubricin on Model Surfaces: Polymer Brush-Like Behavior of a Glycoprotein. Biophys J. 2007; 92:1693–1708. [PubMed: 17142292]
12. Zappone B, Greene GW, Oroudjev E, Jay GD, Israelachvili JN. Molecular Aspects of Boundary Lubrication by Human Lubricin: Effect of Disulfide Bonds and Enzymatic Digestion. Langmuir. 2008; 24:1495–1508. [PubMed: 18067335]
13. Greene GW, Martin LL, Tabor RF, Michalczyk A, Ackland LM, Horn R. Lubricin: A Versatile, Biological Anti-Adhesive with Properties Comparable to Polyethylene Glycol. Biomaterials. 2015; 53:127–136. [PubMed: 25890713]
14. Tirrell M, Patel S, Hadziioannou G. Polymeric Amphiphiles at Solid Fluid Interfaces - Forces between Layers of Adsorbed Block Copolymers. Proc Natl Acad Sci U S A. 1987; 84:4725–4728.
15. Eiser E, Klein J, Witten TA, Fetters LJ. Shear of Telechelic Brushes. Phys Rev Lett. 1999; 82:5076–5079.
16. Dalsin JL, Hu BH, Lee BP, Messersmith PB. Mussel Adhesive Protein Mimetic Polymers for the Preparation of Nonfouling Surfaces. J Am Chem Soc. 2003; 125:4253–4258. [PubMed: 12670247]
17. Lee H, Scherer NF, Messersmith PB. Single-Molecule Mechanics of Mussel Adhesion. Proc Natl Acad Sci U S A. 2006; 103:12999–13003. [PubMed: 16920796]
18. Lee H, Dellatore SM, Miller WM, Messersmith PB. Mussel-Inspired Surface Chemistry for Multifunctional Coatings. Science. 2007; 318:426–430. [PubMed: 17947576]
19. Zhao H, Waite JH. Linking Adhesive and Structural Proteins in the Attachment Plaque of Mytilus Californianus. J Biol Chem. 2006; 281:26150–26158. [PubMed: 16844688]
20. Heo J, Kang T, Jang SG, Hwang DS, Spruell JM, Killops KL, Waite JH, Hawker CJ. Improved Performance of Protected Catecholic Polysiloxanes for Bioinspired Wet Adhesion to Surface Oxides. J Am Chem Soc. 2012; 134:20139–20145. [PubMed: 23181614]
21. Kang T, Amir RJ, Khan A, Ohshimizu K, Hunt JN, Sivanandan K, Montanez MI, Malkoch M, Ueda M, Hawker CJ. Facile Access to Internally Functionalized Dendrimers through Efficient and Orthogonal Click Reactions. Chem Commun. 2010; 46:1556–1558.
22. Hadziioannou G, Patel S, Granick S, Tirrell M. Forces between Surfaces of Block Copolymers Adsorbed on Mica. J Am Chem Soc. 1986; 108:2869–2876.
23. Taunton HJ, Toprakcioglu C, Fetters LJ, Klein J. Forces between Surfaces Bearing Terminally Anchored Polymer-Chains in Good Solvents. Nature. 1988; 332:712–714.
24. de Gennes PG. Physique Des Surfaces Et Des Interfaces -Stabilité De Films Polymére/Solvant. C R Acad Sci Série 2. 1985; 300:839–843.
25. Marzolin C, Auroy P, Deruelle M, Folkers JP, Leger L, Menelle A. Neutron Reflectometry Study of the Segment-Density Profiles in End-Grafted and Irreversibly Adsorbed Layers of Polymer in Good Solvents. Macromolecules. 2001; 34:8694–8700.
26. Alonzo J, Mays JW, Kilbey SM II. Forces of Interaction between Surfaces Bearing Looped Polymer Brushes in Good Solvent. Soft Matter. 2009; 5:1897–1904.
27. Yu J, Wei W, Danner E, Israelachvili JN, Waite JH. Effects of Interfacial Redox in Mussel Adhesive Protein Films on Mica. Adv Mater. 2011; 23:2362–2366. [PubMed: 21520458]
28. Muller M, Lee S, Spikes HA, Spencer ND. The Influence of Molecular Architecture on the Macroscopic Lubrication Properties of the Brush-Like Co-Polyelectrolyte Poly(L-Lysine)-G-Poly(Ethylene Glycol) (Pll-G-Peg) Adsorbed on Oxide Surfaces. Tribol Lett. 2003; 15:395–405.
29. Raviv U, Frey J, Sak R, Laurat P, Tadmor R, Klein J. Properties and Interactions of Physigrafted End-Functionalized Poly(Ethylene Glycol) Layers. Langmuir. 2002; 18:7482–7495.
30. Sudo H, Kodama HA, Amagai Y, Yamamoto S, Kasai S. In Vitro Differentiation and Calcification in a New Clonal Osteogenic Cell Line Derived from Newborn Mouse Calvaria. J Cell Biol. 1983; 96:191–198. [PubMed: 6826647]
31. Tominaga H, Ishiyama M, Ohseto F, Sasamoto K, Hamamoto T, Suzuki K, Watanabe M. A Water-Soluble Tetrazolium Salt Useful for Colorimetric Cell Viability Assay. Anal Commun. 1999; 36:47–50.

32. Hwang DS, Gim Y, Kang DG, Kim YK, Cha HJ. Recombinant Mussel Adhesive Protein Mgfp-5 as Cell Adhesion Biomaterial. J Biotechnol. 2007; 127:727–735. [PubMed: 16979252]
33. Israelachvili J, Min Y, Akbulut M, Alig A, Carver G, Greene W, Kristiansen K, Meyer E, Pesika N, Rosenberg K. Recent Advances in the Surface Forces Apparatus (Sfa) Technique. Rep Prog Phys. 2010; 73:036601.
34. Israelachvili JN. Thin-Film Studies Using Multiple-Beam Interferometry. J Colloid Interface Sci. 1973; 44:259–272.
35. Israelachvili JN, Adams GE. Measurement of Forces between 2 Mica Surfaces in Aqueous Electrolyte Solutions in Range 0–100 Nm. J Chem Soc Faraday Trans 1. 1978; 74:975.
36. Marra J, Israelachvili J. Direct Measurements of Forces between Phosphatidylcholine and Phosphatidylethanolamine Bilayers in Aqueous-Electrolyte Solutions. Biochemistry. 1985; 24:4608–4618. [PubMed: 4063343]
37. Israelachvili, JN. Intermolecular & Surface Forces. 3. Elsevier Academic Press; San Diego, CA: 2011.
38. Horn RG, Israelachvili JN, Pribac F. Measurement of the Deformation and Adhesion of Solids in Contact. J Colloid Interface Sci. 1987; 115:480–492.
39. Stöhr, J. NEXAFS Spectroscopy. 1. Springer; Berlin: 1996. p. xvp. 403
40. Harris M, Appel G, Ade H. Surface Morphology of Annealed Polystyrene and Poly(Methyl Methacrylate) Thin Film Blends and Bilayers. Macromolecules. 2003; 36:3307–3314.

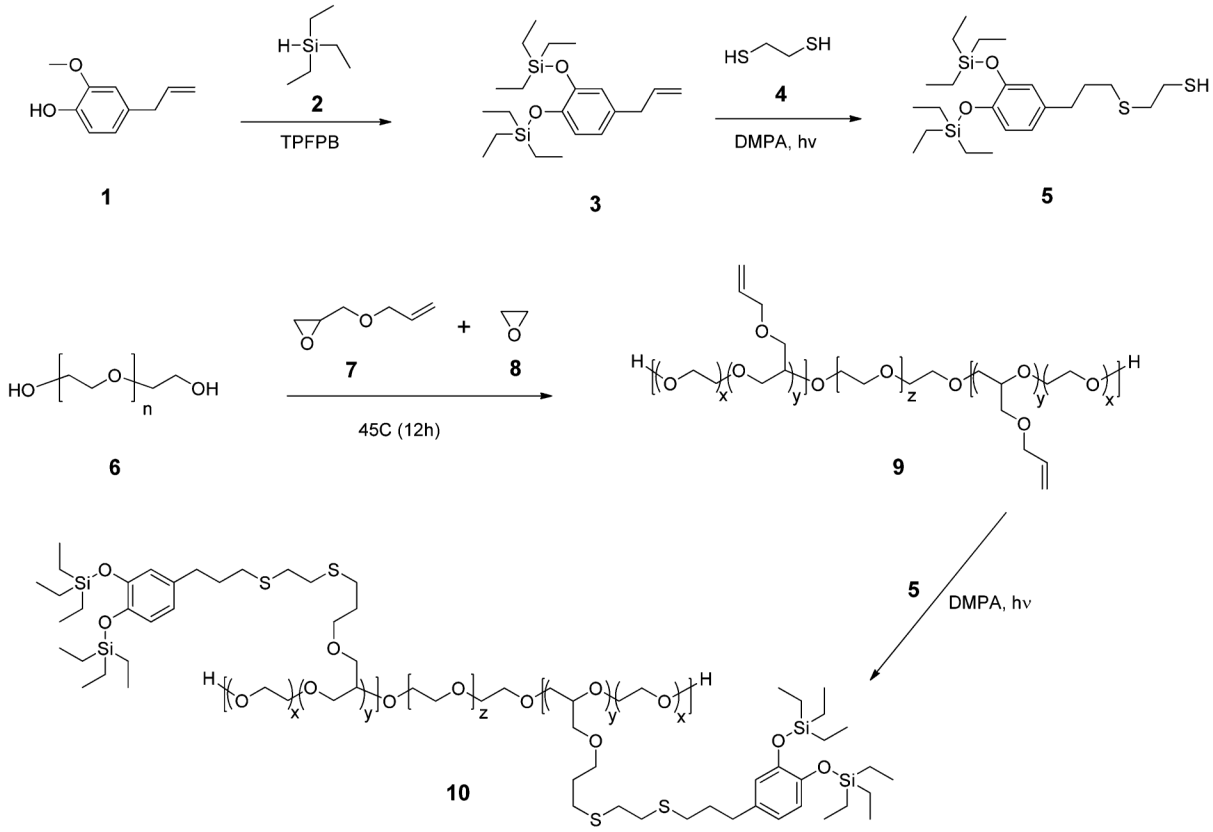

Figure 1.
Synthetic strategy of silyl-protected catecholic monomer and catechol-functionalized poly(ethylene glycol) triblock copolymer.

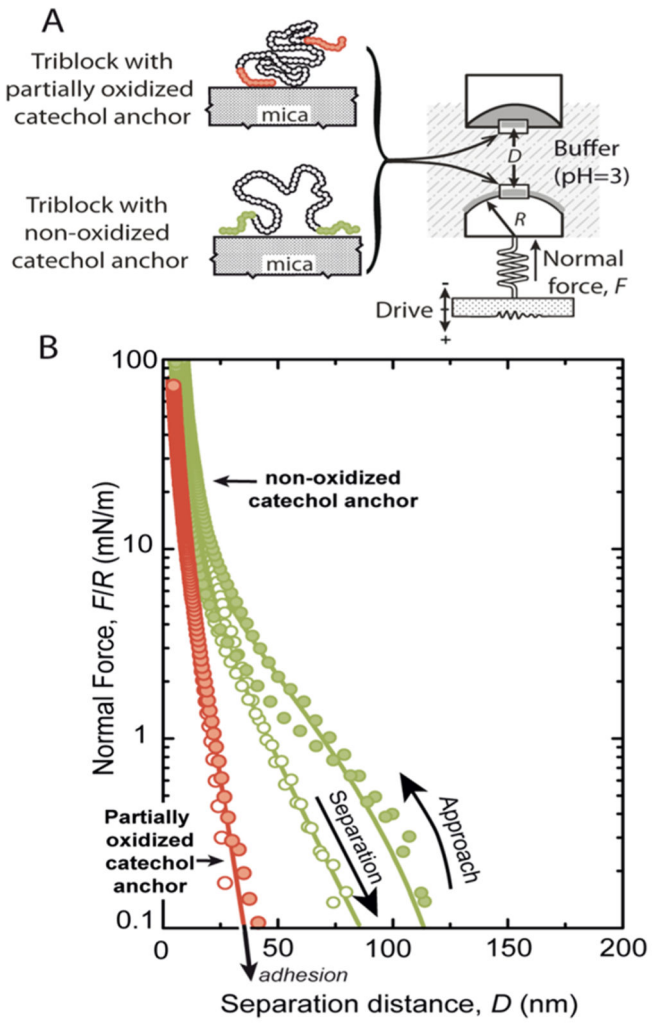

Figure 2.

SFA-based measurement of repulsive and attractive forces in symmetric films of catechol-anchored polymer loops on mica. (A) Schematic representation of the SFA setup used to measure the interactions. (B) Interaction forces measured in acetate buffer (pH 3) between two mica surfaces coated with PEO triblock copolymer adsorbed at pH 3 (nonoxidized catechol) or 5 (partially oxidized catechol). When the polymer is adsorbed at pH 3, the force profile shows a brush-like behavior of the polymer layer with no adhesion, which is indicative of the presence of a high surface density of loops. When the polymer is adsorbed at pH 5, the interaction force curve is purely exponential, which is characteristic of a random coil (or mushroom) conformation of the polymer. Adhesion between the surfaces indicates that the surfaces are not fully covered by the polymer and that polymer bridges are formed. Solid lines are fits to eq 1.

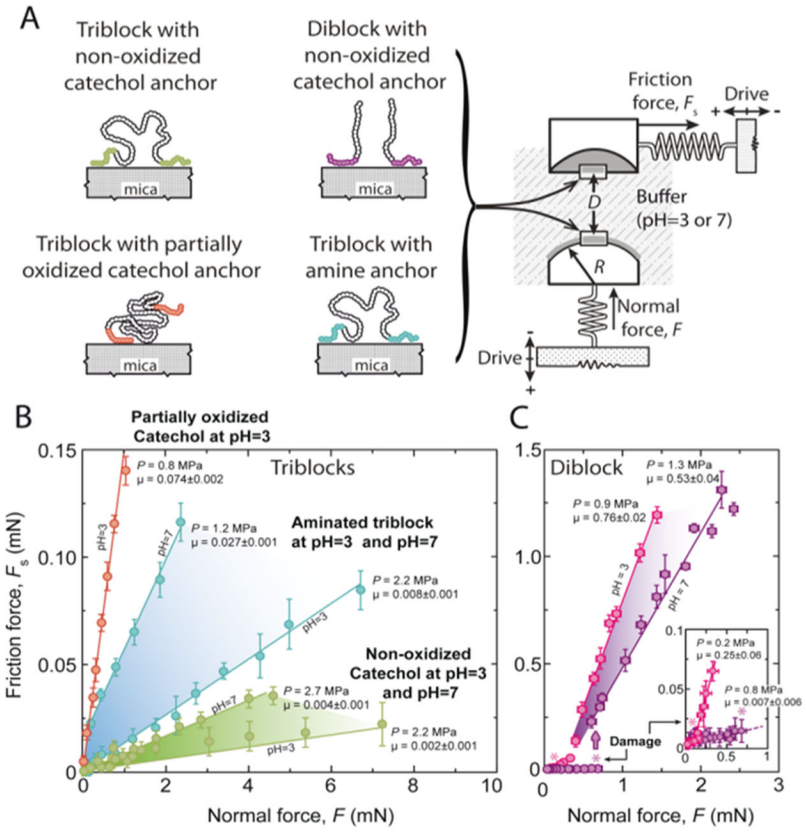

Figure 3.

Tribological testing of triblock polymer and the impact of the conformation on polymer performance. (A) Schematic of the testing configuration together with the different triblock copolymers adsorbed on the mica substrate. (B) Friction forces between two mica surfaces bearing triblock copolymer chains with catechol, partially oxidized catechol, or amine anchor groups. (C) Lubricating properties of neutral polymer brushes of similar length show excellent lubricating properties up to a certain applied normal force above which friction forces increase dramatically.

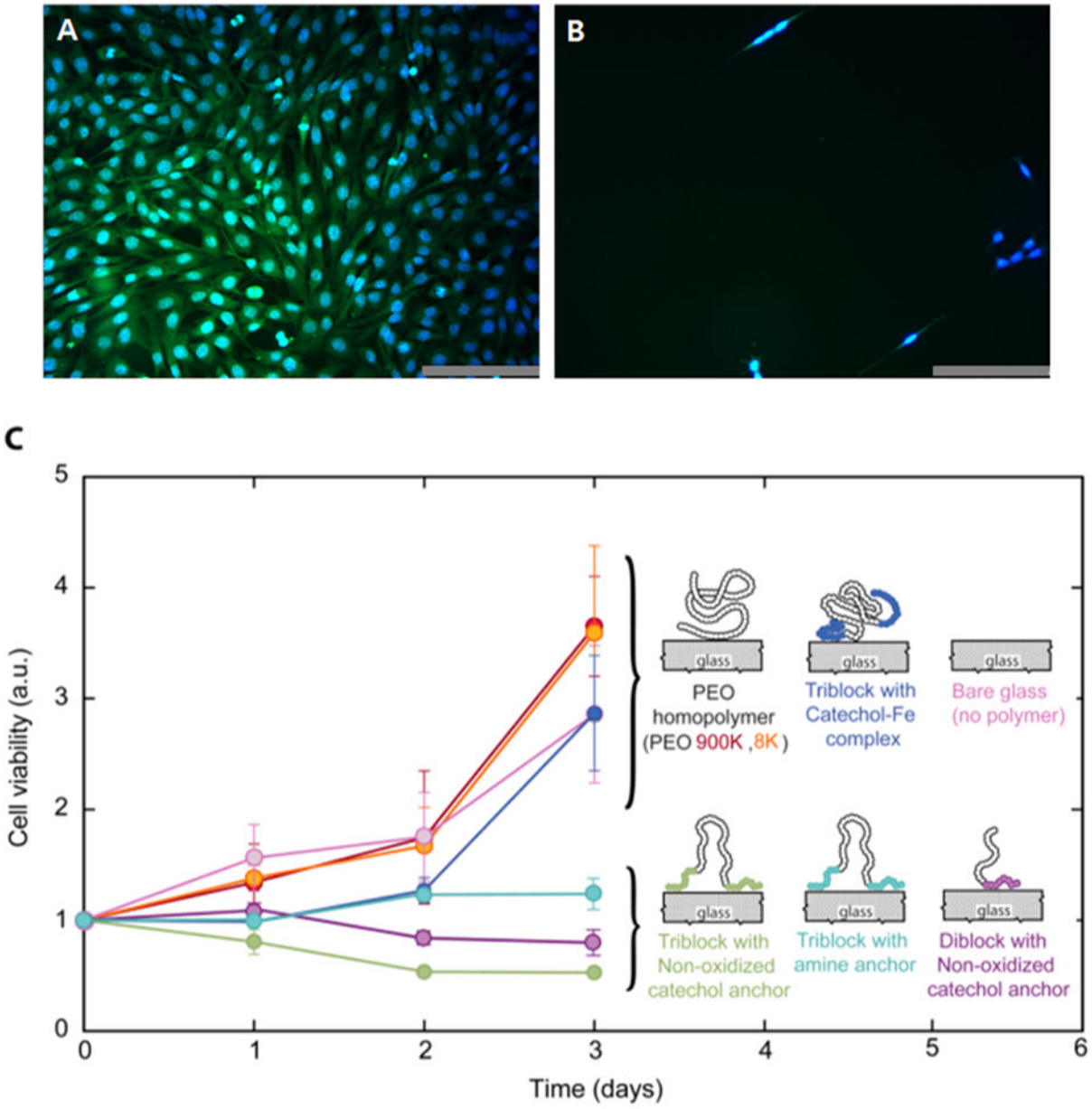

Figure 4.

MC-3T3 cell adhesion assay on (A) bare glass and (B) glass coated with catechol-functionalized triblock copolymer. (C) Comparison of the MC-3T3 cell proliferation on bare glass (pink) and catechol-functionalized triblock copolymer (green), PEO 900k (red), PEO 8k (orange), triblock copolymer–Fe^{3+} (blue), diblock coplymer (purple)-coated glasses for 3 days. Initial cell viability (0 day) after cell seeding was normalized as 1. Each value and error bar represents the mean of triplicate samples and its standard deviation. Scale bar = 100 μm.